Spin- and charge-excitation gaps in the one-dimensional periodic Anderson model

Nishino, Tomotoshi

Ueda, Kazuo

(Citation)
Physical Review B,47(19):12451-12458

(Issue Date)
1993-05-15

(Resource Type)
journal article

(Version)
Version of Record

(URL)
https://hdl.handle.net/20.500.14094/90001233

Spin- and charge-excitation gaps in the one-dimensional periodic Anderson model

T. Nishino
Physics Department, College of General Education, Tohoku University, Sendai 980, Japan
and Paul Scherrer Institut, 5232 Villigen PSI, Switzerland

Kazuo Ueda*
Paul Scherrer Institut, 5232 Villigen PSI, Switzerland
(Received 7 December 1992)

Spin and charge excitations in the one-dimensional periodic Anderson model at half filling are studied in the entire range of the Coulomb interaction U. It is confirmed by exact numerical diagonalization of up to eight sites that an excitation gap exists for any U. In the strong-coupling region, both the spin-excitation gap Δ_s and charge-excitation gap Δ_c decrease with increasing U. A finite-size scaling shows that Δ_s decreases exponentially as a function of U which is consistent with the spin gap in the Kondo-lattice model. The charge gap Δ_c decreases much more slowly than the spin gap. The ratio between the two gaps, $R=\Delta_c/\Delta_s$, increases monotonically from unity and diverges in the strong-coupling limit: it appears to be a useful quantity for measuring the strength of electron correlation in a Kondo insulator.

I. INTRODUCTION

A new class of materials , the "Kondo insulators," has attracted much interest from condensed-matter physicists.[1-3] The periodic Anderson model (PAM) at half filling is an obvious candidate as a theoretical model for the Kondo insulator, since there exists a hybridization gap at least for the noninteracting case. In this paper, we will examine the ground-state properties of the simplest PAM, which neglects the orbital degeneracy

$$H=H_0+H_I ,$$
$$H_0=-t\sum_{i,\tau,\sigma} c_{i\sigma}^{\dagger}c_{i+\tau\sigma}-V\sum_{i,\sigma}(c_{i\sigma}^{\dagger}f_{i\sigma}+f_{i\sigma}^{\dagger}c_{i\sigma}) , \tag{1.1}$$
$$H_I=U\sum_i (f_{i\uparrow}^{\dagger}f_{i\uparrow}-\tfrac{1}{2})(f_{i\downarrow}^{\dagger}f_{i\downarrow}-\tfrac{1}{2}) ,$$

where $c_{i\sigma}^{\dagger}$ creates a conduction electron of spin σ at site i and $f_{i\sigma}^{\dagger}$ creates a local f electron. The summation with respect to τ is taken over nearest-neighbor sites. The mixing between the conduction band and the f orbital is given by V, and the intra-atomic Coulomb repulsion in the f orbital is U. In the present form the symmetric condition is assumed, which keeps the number of f electrons at strictly one per site.

Recently it was proved rigorously that the ground state of the symmetric PAM at half filling is a singlet for any interaction strength.[4] However, the theorem is not powerful enough to determine when the model describes a Kondo insulator. The most important feature of the Kondo insulator is that the ground state is a singlet with a gap for every type of excitation. Therefore the question is related to the existence or absence of long-range order: if there is long-range order which breaks a continuous symmetry, then there are gapless Goldstone modes. Of course, in one dimension there is no long-range order even in the ground state, except for a ferromagnetic order. However, the finite excitation gap leads to an exponential decay of correlation functions, while gapless excitations lead to a power-law decay.

In the strong-coupling limit, the PAM is mapped to the Kondo-lattice model (KLM). For the one-dimensional KLM with a half-filled conduction band, Tsunetsugu *et al.* have shown that the spin-excitation gap is always finite (the charge gap is larger than the spin gap), and that therefore the ground state is an incompressible spin liquid for any nonzero exchange coupling.[5] On the other hand, for a weak Coulomb interaction, the PAM has a hybridization gap. Thus it is natural to expect that the PAM at half filling can be used as a theoretical model for the Kondo insulator at least in one dimension. In this paper, we will study the one-dimensional PAM at half filling by numerical exact diagonalization, and show that its ground state is a spin liquid state for any interaction U.

Since there is no level crossing for the ground state, the nature of the spin liquid state changes continuously as a function of the interaction constant. However, the spin liquid state in the large-U limit, which may be called a Kondo insulating state, is quite different from the noninteracting case which may be called a hybridization gap state. What is a good quantity which characterizes this difference? For this measure, we propose the ratio of the charge gap to the spin gap because, as a function of U, it increases monotonically from unity in the noninteracting case and diverges in the large-U limit.

The present paper is organized as follows. In Sec. II, we discuss several analytical approaches for the elementary excitations as a reference for subsequent discussions on numerical results. We first define spin and charge excitations using the $SO(4)$ symmetry of the symmetric PAM. We then evaluate the charge gap Δ_c and the spin gap Δ_s in the small-U region by considering scattering of an excited particle-hole pair (the excitonic effect). For the large-U region, we use the Gutzwiller and the Hartree-Fock approximations, which offer different

viewpoints. In Sec. III, we show results of exact diagonalization and compare them with the analytical predictions and also with the corresponding quantities in the KLM. By using a finite-size scaling, the asymptotic behavior of the spin and charge gaps in the strong-coupling region is discussed. Finally, we summarize the results in Sec. IV.

II. PROPERTIES OF EXCITATIONS

The principal aim of this paper is to study the nature of spin and charge excitations from the spin liquid ground state of the half-filled PAM. Charge excitations are generally coupled with spin excitations, and it is not trivial to define the charge- and spin-excitation gaps separately. However, for the symmetric PAM, we can define them without ambiguity with the help of its $SO(4)$ symmetry. In Sec. II A, we briefly summarize $SO(4)$ symmetry and present the definition of the spin and charge excitations. Several approximate treatments are possible for these excitations. In Sec. II B, we study properties of these excitations in the weak-coupling region by considering only single-particle-hole pair excitations. Subsequently, in Sec. II C, the strong-coupling region is discussed on the basis of the Gutzwiller theory and the Hartree-Fock–RPA approximation.

A. $SO(4)$ symmetry

It is well known that the Hubbard model has $SO(4)$ symmetry,[6,7] which consists of two independent $SU(2)$ symmetries in spin and pseudospin space: the latter is for the charge degrees of freedom. The PAM can be viewed as a generalized Hubbard model which has a special connectivity and a site-dependent Coulomb interaction. Thus the symmetric PAM also has $SO(4)$ symmetry if the lattice is bipartite.[8]

Existence of $SO(4)$ symmetry is easily shown as follows. The Hamiltonian is invariant under the spin rotation, so that the model has ordinary $SU(2)$ symmetry in spin space, where the generators of rotations are the spin operators:

$$\begin{aligned} S^z &= \tfrac{1}{2}\sum_i (c_{i\uparrow}^\dagger c_{i\uparrow} - c_{i\downarrow}^\dagger c_{i\downarrow} + f_{i\uparrow}^\dagger f_{i\uparrow} - f_{i\downarrow}^\dagger f_{i\downarrow}) , \\ S^+ &= \sum_i (c_{i\uparrow}^\dagger c_{i\downarrow} + f_{i\uparrow}^\dagger f_{i\downarrow}) , \\ S^- &= \sum_i (c_{i\downarrow}^\dagger c_{i\uparrow} + f_{i\downarrow}^\dagger f_{i\uparrow}) . \end{aligned} \tag{2.1}$$

Another $SU(2)$ symmetry—a hidden symmetry—is obtained through a particle-hole transformation[9] for one species of the spin, say down,

$$\begin{aligned} c_{i\downarrow} &\rightarrow (-1)^i c_{i\downarrow}^\dagger , \\ f_{i\downarrow} &\rightarrow -(-1)^i f_{i\downarrow}^\dagger . \end{aligned} \tag{2.2}$$

By this canonical transformation, a positive-U symmetric PAM maps onto a negative-U one. The negative-U PAM also has rotational symmetry in its spin space. Therefore the original positive-U PAM has another $SU(2)$ symmetry represented by the following operators, which are derived by the transformation from the spin operators given by Eq. (2.1):[10]

$$\begin{aligned} J^z &= \tfrac{1}{2}\sum_i (c_{i\uparrow}^\dagger c_{i\uparrow} + c_{i\downarrow}^\dagger c_{i\downarrow} + f_{i\uparrow}^\dagger f_{i\uparrow} + f_{i\downarrow}^\dagger f_{i\downarrow} - 2) , \\ J^+ &= \sum_i (-1)^i (c_{i\uparrow}^\dagger c_{i\downarrow}^\dagger - f_{i\uparrow}^\dagger f_{i\downarrow}^\dagger) , \\ J^- &= \sum_i (-1)^i (c_{i\downarrow} c_{i\uparrow} - f_{i\downarrow} f_{i\uparrow}) . \end{aligned} \tag{2.3}$$

These operators are often called pseudospin operators. Note that the z component of the pseudospin operators is nothing but the charge operator.

We can now classify all states of the half-filled symmetric PAM by using quantum numbers S and J. Since the ground state is spin singlet ($S=0$) for both positive and negative U, it is also pseudospin singlet ($J=0$).[4] We can define spin excitations generally by the excitations which change the quantum number S. This definition is naturally understood when we consider the dynamical spin susceptibility (at $T=0$, for simplicity),

$$\chi_{zz}(q,w) = \sum_j \left[\frac{|\langle 0|S_{zq}|j\rangle|^2}{w - w_{j0} + i\eta} - \frac{|\langle j|S_{zq}|0\rangle|^2}{w - w_{j0} + i\eta} \right] , \tag{2.4}$$

where S_{zq} is a Fourier transform of the spin operator, and $|j\rangle$ is an excited state and w_{j0} is its excitation energy. It can be readily seen that only those excited states with $S=1$ and $J=0$ contribute to the spin susceptibility at $T=0$. Similarly charge excitations are defined generally by those excitations which accompany a change in J. Only excitations to states with $S=0$ and $J=1$ contribute to the charge susceptibility in the ground state.

As we will show, the lowest spin-excited state has $S=1$ and $J=0$, and the lowest charge-excited state has $S=0$ and $J=1$. Therefore we define the spin- and charge-excitation gaps by

$$\Delta_s = E_0(S=1,J=0) - E_0(S=0,J=0) \tag{2.5}$$

and

$$\Delta_c = E_0(S=0,J=1) - E_0(S=0,J=0) , \tag{2.6}$$

respectively, where $E_0(S,J)$ is the lowest energy in the subspace specified by S and J. In general, there is another group of excited states that have different sets of S and J: excitations to the states which correspond to composite states of spin and/or charge excitations. However, these states usually have higher excitation energies compared with the bare spin or charge excitations.

Before closing this subsection, we briefly touch on the symmetry of the Kondo-lattice model. The KLM can be derived from the symmetric PAM through the Schrieffer-Wolff transformation, leading to an antiferromagnetic exchange interaction J_K.[11] Since this transformation conserves the rotational symmetries in the spin and pseudospin spaces, the KLM also has $SO(4)$ symmetry. $SO(4)$ symmetry in the KLM can be derived more directly through the particle-hole transformation defined by Eq. (2.2); the KLM maps onto the so-called

"attractive-J_K model"[12] that is also invariant under spin rotations. Thus both the KLM and the attractive-J_K model have $SU(2)$ symmetries in spin and pseudospin spaces. It is clear that $SO(4)$ symmetry also exists for the ferromagnetic KLM, which is a coupled spin-electron model for the Haldane gap state.[5]

B. Excitations in the weak-coupling region

We start from the noninteracting case $U=0$. In this limit, we can diagonalize the Hamiltonian as

$$H_0=\sum_{k\sigma}(\lambda_k^- a_{k\sigma}^\dagger a_{k\sigma}+\lambda_k^+ b_{k\sigma}^\dagger b_{k\sigma}) \tag{2.7}$$

with

$$\lambda_k^\pm=\tfrac{1}{2}(\varepsilon_k\pm\sqrt{\varepsilon_k^2+4V^2}) \tag{2.8}$$

by using the canonical transformation

$$\begin{aligned} a_{k\sigma}&=\cos\theta_k c_{k\sigma}+\sin\theta_k f_{k\sigma}\ , \\ b_{k\sigma}&=\sin\theta_k c_{k\sigma}-\cos\theta_k f_{k\sigma}\ , \end{aligned} \tag{2.9}$$

where the mixing angle θ_k is given by $\cos^2\theta_k=\frac{1}{2}(1-\varepsilon_k/\sqrt{\varepsilon_k^2+4V^2})$. For the one-dimensional case, the dispersion of the conduction band is $\varepsilon_k=-2t\cos k$. The ground state of the half-filled PAM at $U=0$ is just a filled band state of a particles $|\phi_0\rangle=\prod_{k\sigma}\alpha_{k\sigma}^\dagger|0\rangle$.

The lowest spin excitation is constructed by a particle-hole pair excitation with spin flip, $b_{0\uparrow}^\dagger a_{\pi\downarrow}|\phi_0\rangle$. This state has $S=1$, $S_z=1$, and $J=0$, and total momentum π. The other states in the spin triplet are obtained by successive operations of S^- as usual. One of the lowest charge-excited states is given by the image of the spin-excited state through the particle-hole transformation Eq. (2.2), $b_{0\uparrow}^\dagger b_{0\downarrow}^\dagger|\phi_0\rangle$. This state has $S=0$, $J=1$, and $J_z=1$. The other states in the pseudospin triplet are obtained by applying J^-. The states with $J_z=\pm1$ have a total momentum zero, while the $J_z=0$ state has a total momentum π. Since $\lambda_0^+=-\lambda_\pi^-$, both Δ_s and Δ_c are equal to the hybridization gap $\lambda_0^+-\lambda_\pi^-$.

When U is smaller than the hybridization gap, it is sufficient to consider only the states with one particle-hole pair. Therefore the problem reduces to a two-particle problem in the subspace spanned by $|p,q\rangle=b_{p\uparrow}^\dagger a_{q\downarrow}|\phi_0\rangle$. These states have $S_z=1$ and total momentum $p-q$. Matrix elements are calculated as

$$\begin{aligned} &\langle p,q|H|p,q\rangle=\langle\phi_0|H_0|\phi_0\rangle+\lambda_p^+-\lambda_q^--LU/4\ , \\ &\langle p+k,q+k|H_I|p,q\rangle \\ &\qquad=-\frac{U}{N}\cos\theta_{p+k}\cos\theta_p\sin\theta_{q+k}\sin\theta_q\ , \end{aligned} \tag{2.10}$$

where L is the number of lattice sites.

Now we diagonalize the Hamiltonian in the restricted Hilbert space to obtain the spin gap. Because of the translational symmetry, an eigenstate has the form $|\Psi_K\rangle=\sum_k w_k|k,k-K\rangle$, where the mixing weight w_k is determined through a Schrödinger equation:

$$\begin{aligned} E_K w_k=(\lambda_k^+-\lambda_{k-K})w_k-\frac{U}{N}\cos\theta_k\sin\theta_{k-K} \\ \times\sum_{k'}w_{k'}\cos\theta_{k'}\sin\theta_{k'-K}\ . \end{aligned} \tag{2.11}$$

Here we take $\langle\phi_0|H_0|\phi_0\rangle$ as the origin of the energy eigenvalue E_K. The equation has essentially the same form as the integral equation which appears in Kanamori's t-matrix approximation.[13] One can solve the equation by multiplying w_k on both sides of Eq. (2.11) and summing up with respect to index k:

$$-\frac{1}{U}=\frac{1}{N}\sum_k\frac{\cos^2\theta_k\sin^2\theta_{k-K}}{E_K-\lambda_k^++\lambda_{k-K}^-}\ . \tag{2.12}$$

The equation shows that an excitonic level appears in the middle of the band gap. The "exciton energy" E_K has its minimum at $K=\pi$. It is easy to see that the spin excitation gap $\Delta_s=E_\pi$ is a decreasing function of U. The functional form of E_K near $U=0$ depends on the density of states of $\lambda_k^\pm$. If the system size is finite, then Δ_s decreases linearly with U, because the distribution of $\lambda_k^\pm$ is discrete. In the limit of $L\to\infty$, the linear dependence changes into a U^2 dependence.

Finally we consider Δ_c in the weak-coupling region. We can obtain the expression for Δ_c by using the particle-hole transformation [Eq. (2.2)]:

$$\frac{1}{U}=\frac{1}{N}\sum_k\frac{\cos^2\theta_k\sin^2\theta_{k-K}}{E_K-\lambda_k^++\lambda_{k-K}^-}\ , \tag{2.13}$$

where E_K represents an eigenvalue of a charge-excited state with momentum $\pi-K$. In contrast to the spin excitation, the lowest-energy state with $J_z=1$ is a scattering state with zero total momentum. Again, the functional form of Δ_c depends on the distribution of $\lambda_k^\pm$. If the system size is finite, then Δ_c increases linearly with U, with the same slope as Δ_s decreases. On the other hand, Δ_c of any infinite system remains the same as the band gap $\lambda_0^+-\lambda_\pi^-$ within the present approximation.

C. Excitations in the strong-coupling region

Another limiting case for the PAM is $U=\infty$; the f spins are completely isolated from the conduction band, and the ground state at half filling is 2^L-fold degenerate. Both Δ_s and Δ_c are zero in this case, but the limit of their ratio $R=\Delta_c/\Delta_s$ has to be determined. A perturbation expansion from $U=\infty$ does not give R immediately. The strong-coupling expansion on the PAM gives the KLM as its effective Hamiltonian, but the ratio in the KLM has not been studied. Here we employ two frequently used approximations, i.e., the Gutzwiller approximation[14] and the Hartree-Fock–random-phase-approximation (HF-RPA).

In the Gutzwiller approximation,[14] the effect of the Coulomb repulsion is represented by a suppression of electron itineracy.[15] The method was applied to the PAM by Rice and Ueda.[16] Their result was reformulated by Kotliar and Ruckenstein by using a slave-boson

mean-field approach.[17,18] The Gutzwiller approximation replaces the hybridization parameter V in Eq. (1.1) by an effective one,

$$V_{\text{eff}}=2d\sqrt{2-4d^2}V\ , \tag{2.14}$$

where d^2 is given by the averaged probability for double occupancy $\langle f_{i\uparrow}^{\dagger}f_{i\uparrow}f_{i\downarrow}^{\dagger}f_{i\downarrow}\rangle$. The "variational" ground-state energy at half filling is given by the minimum of

$$E=\sum_{k\sigma}\lambda_{k\sigma}^{-}(V_{\text{eff}})+U\sum_{i}(d^2-\tfrac{1}{4}) \tag{2.15}$$

with respect to d^2, where $\lambda_k^{-}(V_{\text{eff}})=\frac{1}{2}(\varepsilon_k-\sqrt{\varepsilon_k^2+4V_{\text{eff}}^2})$ is the quasiparticle energy with the effective hybridization. The paramagnetic Gutzwiller approximation does not change the basic band structure, thereby the approximation gives the same value for Δ_s and Δ_c:

$$\Delta_s=\Delta_c=2\sqrt{t^2+V_{\text{eff}}^2}-2t\ . \tag{2.16}$$

The asymptotic form of $\Delta_{s(c)}$ of the one-dimensional PAM is given by[16]

$$\Delta_{s(c)}=\frac{V_{\text{eff}}^2}{t}=\pi^2 t\exp\left[-\frac{\pi tU}{8V^2}\right] \tag{2.17}$$

in the large-U region.

The Gutzwiller approximation predicts the same Δ_s and Δ_c which decrease exponentially with U in any dimension.[19] However, it should be noted that in the Gutzwiller approximation the effect of strong electron-electron correlation is taken into account only through the reduction of the mixing matrix element, and the probability of doubly occupied f states is not really suppressed in the resultant wave function. This is the reason why the two gaps are the same in the Gutzwiller approximation. This causes a problem in a discussion of excitations. To be explicit, let us consider the spin excitation with $S_z=1$. The spin excitation is described by a particle-hole pair excitation, both of which have strong-f character. The Gutzwilller projection modifies the extended particle-hole pair excitation to a linear combination of spin-flip excitations of a localized f spin. The problem for the charge excitations is more serious. Now we take the example of the $J_z=1$ state. To create this excitation, two particles of mostly f character are added to the ground-state wave function. However, the dominant components in this wave function with two additional f electrons should be suppressed by the Gutzwiller projection. Therefore when we proceed further than the Gutzwiller approximation, the following is expected: (1) The form of the spin gap may be different from Eq. (2.17) in the large-U region; and (2) the charge gap is larger than the spin gap.

Now we turn to another approach: the Hartree-Fock (HF) approach. The optimal HF solution of the one-dimensional half-filled PAM is the antiferromagnetic (AF) one. The HF equation in this case is expressed by a 4×4 matrix equation in the momentum space. In the HF approximation, spin and charge excitations are given by single particle-hole pair excitations and $\Delta_s=\Delta_c$. If U is sufficiently large so that the magnetic moment $m=|\langle n_{i\uparrow}\rangle-\langle n_{i\downarrow}\rangle|$ is greater than $\sqrt{2}/U$, then the excitation gap is given by

$$\Delta_c=\Delta_s=(mU/2)\{\sqrt{1+(4V/mU)^2}-1\}\ . \tag{2.18}$$

In the strong-coupling limit, the magnetization m is almost unity and $\Delta_c=\Delta_s$ is proportional to $4V^2/U=J_K/2$, i.e., they are inversely proportional to U. As for the excitations from the HF ground state, we can go further by using the random-phase-approximation. In the RPA, the charge-excitation gap does not change from the HF result, but for the spin excitations it contains spin-wave modes as collective modes in addition to the single-particle-hole excitations. The spin-wave modes are gapless because they are Goldstone modes. Therefore the antiferromagnetic HF-RPA predicts gapless excitations for the spin excitations but a finite excitation gap for the charge excitations. Thus the ratio $R\equiv\Delta_c/\Delta_s$ is divergent in the HF-RPA. The main problem of this approach is the spurious symmetry breaking. However, in the antiferromagnetic HF solution, effects of charge correlation are well taken into account. When we include spin fluctuations around the antiferromagnetic solution in one dimension, the rotational symmetry in the spin space will be restored and the spin excitations will acquire an excitation gap, as is shown for the KLM.[5] Although this nonperturbative effect is crucial for the spin excitations, its effect on the charge excitations is expected to be less important.

The two treatments discussed above give conflicting results for spin and charge excitations. As we discussed already, each of the two approaches has its advantages and disadvantages. In the next section, we will study the spin gap and the charge gap through exact diagonalization. The above discussions are the basis for the analysis of the numerical data in the next section.

III. NUMERICAL RESULTS

We performed the Lanczos diagonalization for the symmetric PAM at half filling up to $L=8$, where L is the number of lattice sites. The translational invariance of the system is employed to reduce memory space.[20] The boundary condition is chosen so that there is a zero-energy level in the conduction band—$\varepsilon_k=0$ for a certain k. Otherwise the lack of such a level causes a large finite-size effect in the strong-coupling region.[5] Periodic boundary conditions are used for $L=4$ and 8, and the antiperiodic ones for $L=6$.

We choose the hopping parameter t in the Hamiltonian [Eq. (1.1)] as an energy unit. In real heavy Fermion materials, V is small, typically on the order of 0.1. However for such a small V, the excitation gap is extremely small even for U of the order of unity. On the other hand, in the strong-coupling region which is our primary concern, one expects that the excitation gap is a function of V^2/U. Therefore, for convenience, we fix $V=1$ and consider various values of U in the following numerical calculations.

To see the overall features of the excitation gap, in Fig. 1 we show Δ_c and Δ_s of the six-site PAM as a function of U. The spin gap Δ_s, shown by the solid line, decreases with increasing U, while the charge gap Δ_c, shown by the

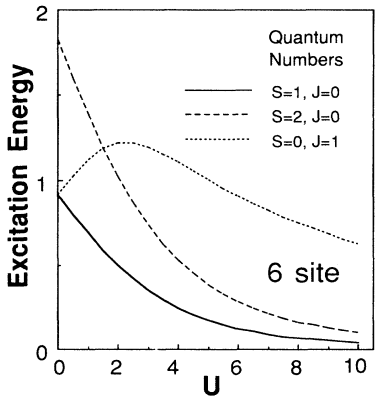

FIG. 1. Elementary excitation energies of various quantum numbers (S,J) in the six-site PAM as a function of U. The solid line is the spin gap Δ_s, while the dotted line the charge gap Δ_c. The double-spin excitation energy is also shown by the dashed line.

dotted line, has its maximum near $U=2$. In the large-U region, Δ_c starts to decrease but is still much larger than Δ_s. In this region, Δ_c is also larger than the double-spin-excitation energy. This example for $L=6$ shows that the ratio $R=\Delta_c/\Delta_s$ increases monotonically as a function of U. In the following, we will discuss the behavior of Δ_c and Δ_s in more detail by also including data for $L=4$ and 8. We start from the spin-excitation gap.

A. Spin-excitation gap

In Fig. 2, we compare numerical Δ_s in the weak-coupling region with the results obtained by the excitonic treatment Eq. (2.12) for the same system size. The good agreement shows that the lowest spin-excited state in the weak-coupling region can be described as an excitonic bound state. Therefore the spin gap is suppressed by the Coulomb repulsion. In an infinite system, the suppression is proportional to U^2, in contrast to the U linear suppression observed in a finite system.

The spin gap in the strong-coupling region decreases with increasing U. To determine the dependence of Δ_s on U from the data for finite systems, a finite-size scaling similar to the one used for the KLM is necessary.[5] The scaling is performed by using the Gutzwiller form as follows. For each Δ_s calculated by exact diagonalization for a certain U and a certain L, we can determine a $V_{\rm eff}$ that gives the same gap for the same L through Eq. (2.16). (In the case of $L=6$, the equation is slightly modified according to the antiperiodic boundary condition.) This in turn determines the "effective Coulomb interaction" $U_{\rm eff}$, which gives the same spin gap in the Gutzwiller approximation for the same L. In this way we can get a mapping from U to $U_{\rm eff}$ for each system size.

Figure 3 shows the result of the finite-size scaling. Although the lines for $L=4$, 6, and 8 do not overlap perfectly—disagreeing due to a remnant finite-size effect present in our scaling procedure—overall agreement is satisfactory. The fact that $U_{\rm eff}$ is linear in U in the strong-coupling region confirms that the spin-excitation gap decays exponentially with increasing U, $\Delta_s \propto e^{-\pi t U/4\alpha V^2}$. In this expression, $\alpha=2$ is the Gutzwiller exponent, while $\alpha=1$ gives the same exponent as the single-impurity Kondo energy. In order to obtain the scaling constant α, we fit each line by $U_{\rm eff}=a+bU$ in the region $2\le U\le 10$. The fitting parameters are listed in Table I. The scaling factor $\alpha=2/b$ are slightly larger than one, which is consistent with the result of the Kondo-lattice model $1.0\le\alpha\le 1.25$, obtained by Tsunetsugu *et al.*[5]

From the analysis, we can conclude that the symmetric periodic Anderson model at half filling always has an excitation gap which is given by the spin gap. The spin gap shows a smooth crossover from the weak-coupling to the strong-coupling region. This crossover is consistent with

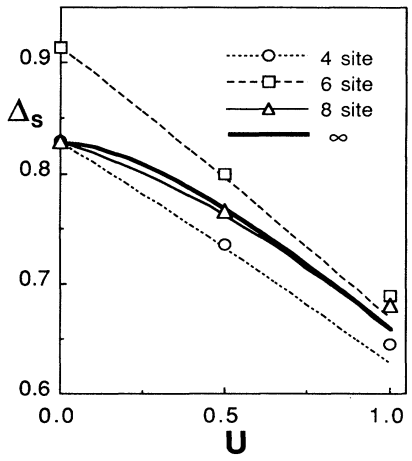

FIG. 2. The spin-excitation energy Δ_s in the weak-coupling region. The open circle, square, and triangle show the numerically calculated spin excitation energies for $L=4$, 6, and 8, respectively. The electron-hole bound-state energy E_π, which is given by Eq. (2.12), is shown by dotted, dashed, solid, and bold lines for $L=4$, 6, 8, and ∞.

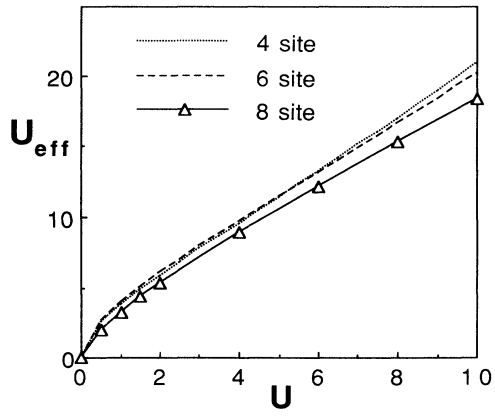

FIG. 3. The finite-size scaling result for Δ_s. The mapping from the Coulomb energy U to the effective one $U_{\rm eff}$ is shown by the dotted and broken lines for $L=4$ and 6, respectively. The results for $L=8$ are shown by the open triangles, for which the solid line is just a guide for the eyes.

TABLE I. Parameters obtained by the linear fitting $U_{\text{eff}}=a+bU$ for each system size. $\alpha=2/b$ is the enhancement factor of the spin gap energy over the single-impurity Kondo energy.

L	a	b	α
4	2.24	1.83	1.10
6	2.63	1.75	1.15
8	2.74	1.56	1.28

the behavior of the spin-correlation functions observed by the quantum Monte Carlo simulations.[21] The spin gap shows an exponential behavior in the strong-coupling region such as the Gutzwiller prediction. The exponent is, however, different from the Gutzwiller theory but still slightly larger than the single-site Kondo energy, indicating a lattice enhancement of the characteristic low-energy scale.

B. Charge-excitation gap

For a finite L, the charge-excitation gap in a weak-coupling region is also well explained by the excitonic treatment discussed in Sec. II B. Figure 4 shows Δ_c in the weak-coupling region. The analytical result agrees well with Δ_c obtained by the numerical diagonalization. It increases linearly in U for a finite system, but the slope vanishes in the limit of $L\rightarrow\infty$.

A transitional behavior from the weak-coupling case to the strong-coupling regime is shown in Fig. 5. For a finite L, after taking a maximum at a certain U, Δ_c decreases with U but much more slowly than Δ_s. In order to find the asymptotic form of Δ_c, we tried various functional forms. The scaling analysis using the Gutzwiller form does not give a good fit for the charge gap, indicating that Δ_c has a different asymptotic form from Δ_s. We found that a simple $1/U$ behavior fits very well for Δ_c, as shown in Fig. 6. Similar behavior is observed for the KLM. Figure 7 shows Δ_c of the PAM and the KLM for $L=8$ as a function of $J_K\equiv 8V^2/U$.[11] The Δ_c is of the KLM (circles) and the PAM (squares) come close to each other in the weak J_K, i.e., in the strong-U region.

The system size dependence of the proportionality constant, $c=\lim_{J\rightarrow 0}(\Delta_c/J)$ is plotted in Fig. 8. Although there is a large finite-size effect for the coefficient, the figure suggests that the proportionality constant c remains finite when extrapolated to the limit of $L=\infty$. Furthermore, it approaches $c=\frac{1}{2}$, which is the prediction of the antiferromagnetic HF treatment discussed in Sec. II C.

Finally we discuss the ratio $R\equiv\Delta_c/\Delta_s$. In the weak-coupling region, the present study has established that for a finite L, Δ_s decreases, while Δ_c increases linearly with U in the weak-coupling region. Therefore, at least for finite L, R is an increasing function of U in the weak-

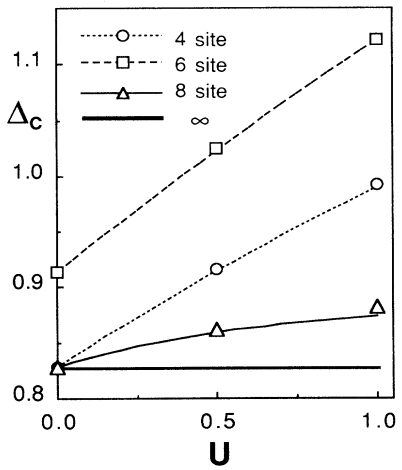

FIG. 4. The charge gap Δ_c in the weak-coupling region. The open circles, squares, and triangles are the results of the exact diagonalization for $L=4$, 6, and 8, respectively. For comparison, the excitation energies E_π given by Eq. (2.13) are shown for $L=4$, 6, 8, and ∞ by dotted, dashed, solid, and bold lines, respectively.

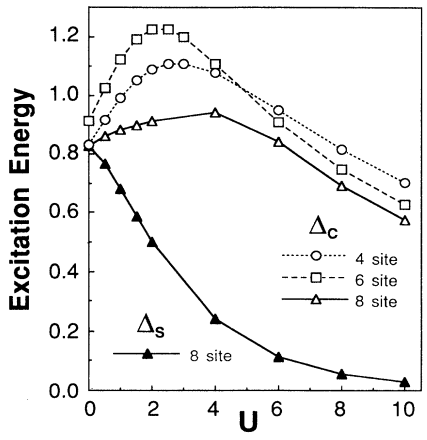

FIG. 5. The charge-excitation energy Δ_c from weak- to strong-coupling regimes for $L=4$ (open circle), 6 (square), and 8 (triangle). The Δ_s for $L=8$ are shown by the filled triangles, for comparison.

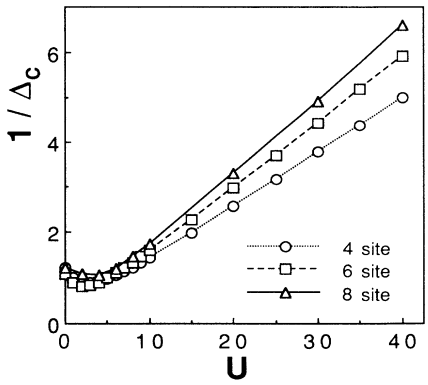

FIG. 6. The asymptotic behavior of Δ_c in the large-U region.

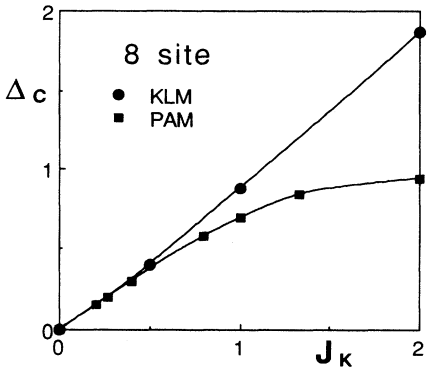

FIG. 7. A comparison of the charge-excitation gaps of KLM and PAM. The horizontal axis is J_K for the KLM and $8V^2/U$ for the PAM.

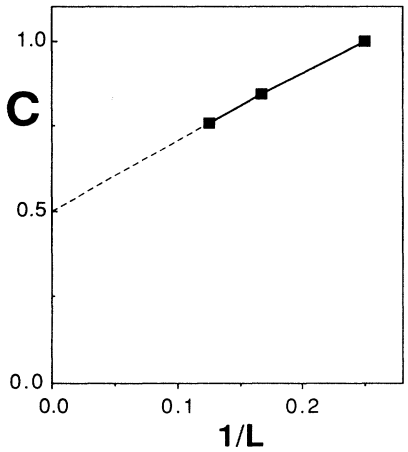

FIG. 8. The system size dependence of the proportional constant of Δ_c with respect to $1/U$. The solid and broken lines are guides for the eyes.

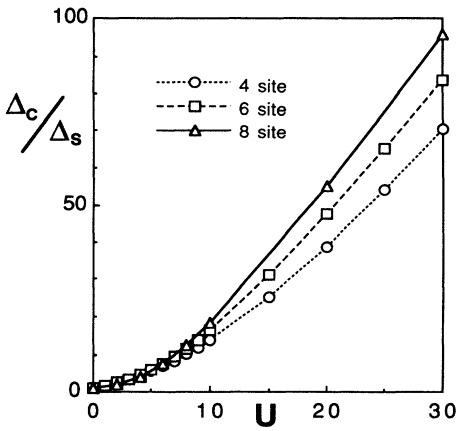

FIG. 9. The ratio between the spin- and charge-excitation gaps, $R \equiv \Delta_c/\Delta_s$.

coupling region. According to Eqs. (2.12) and (2.13), the ratio R also increases in the limit of infinite L, where the deviation from unity is proportional to U^2. Now we turn to the ratio R in the strong-coupling limit. Figure 9 shows the ratio Δ_c/Δ_s up to $U=30$. The ratio increases with U for every L. Moreover, the increasing rate itself is an increasing function of L. Thus we can conclude that Δ_c/Δ_s for $L=\infty$ diverges in the strong-coupling limit.

IV. CONCLUSION AND DISCUSSION

We have calculated the spin- and charge-excitation gaps in the one-dimensional periodic Anderson model at half filling in the entire range of the Coulomb interaction U. It is shown that in the weak-coupling region, the spin-excitation gap Δ_s decreases with increasing U due to the excitonic effect, while the charge-excitation gap Δ_c increases for a finite system. In the strong-coupling region, both Δ_s and Δ_c decrease with U. A finite-size scaling analysis up to $L=8$ shows that Δ_s decreases exponentially as a function of U consistently with the spin gap of the Kondo-lattice model. The charge excitation Δ_c decreases much more slowly than the spin gap, in contrast to the prediction of the Gutzwiller approximation. The numerical results for finite systems up to eight sites are consistent with a $1/U$ dependence of the Δ_c in the strong-coupling region. Still, further study is necessary to determine the functional form of the charge gap in the infinite system. However, concerning the ratio between the two gaps, $R=\Delta_c/\Delta_s$, the present results lead to the conclusion that the ratio diverges in the strong-coupling limit.

Totally different behavior between Δ_c and Δ_s in the strong-coupling region means that a rigid band picture, which appears in various mean-field-type approximations, is a poor description for the excitations. Furthermore, a preliminary numerical calculation of the PAM under finite magnetic fields shows that a large charge-excitation gap remains even when the system has a finite magnetization,[22] another phenomenon which is not explained by the band picture.

The monotonic increase and divergence of R in the strong-coupling limit have important relevance to the clarification of the nature of Kondo insulator materials. It has not been clear what is the basic difference between a strongly correlated Kondo insulator and an insulator due simply to a hybridization gap. The present study indicates that R can be used as a measure of distinguishing the two cases. One remark necessary at this point is that the present model has a high $SO(4)$ symmetry, due to which the charge excitations are unambiguously distinguished from the spin excitations. In a general case with a lower symmetry, there is weak coupling between the two degrees of freedom. However, it may be possible to observe the basic difference between them by looking at, for example, the temperature dependence of the NMR relaxation rate for spin excitations and the optical spectrum for charge excitations. Systematic experimental studies of the spin and charge excitations are highly desirable.

ACKNOWLEDGMENTS

The authors would like to express their sincere thanks to Manfred Sigrist and Hirokazu Tsunetsugu for valuable comments and discussions. Most of the numerical calculations were done on the SX-3 in Centro Svizzero di Calcolo Scientifico (CSCS). The present work was partially supported by a Grant-in-Aid from the Ministry of Education, Science and Culture of Japan, and also the Computation Center of Osaka University.

*Permanent address: Institute of Materials Science, University of Tsukuba, 305 Tsukuba, Japan.

[1]T. Takabatake, Y. Nakazawa, and M. Ishikawa, Jpn J. Appl. Phys. Suppl. **26**, 547 (1987).
[2]M. F. Hundley, P. C. Canfield, J. D. Thompson, Z. Fisk, and J. M. Lawrence, Phys. Rev. B **42**, 6842 (1990).
[3]M. Kasaya, F. Iga, K, Negishi, S. Nakai, and T. Kasuya, J. Magn. Magn. Mater. **31-34**, 437 (1983).
[4]K. Ueda, H. Tsunetsugu, and M. Sigrist, Phys. Rev. Lett. **68**, 1030 (1992).
[5]H. Tsunetsugu, Y. Hatsugai, K. Ueda, and M. Sigrist, Phys. Rev. B **46**, 3175 (1992).
[6]S. C. Zhang, Phys. Rev. Lett. **65**, 120 (1990).
[7]C. N. Yang and S. C. Zhang, Mod. Phys. Lett. B **4**, 759 (1990).
[8]E. H. Lieb, Phys. Rev. Lett. **62**, 1201 (1989).
[9]E. H. Lieb and F. Y. Wu, Phys. Rev. Lett. **20**, 1445 (1968).
[10]R. R. P. Singh and R. T. Scalettar, Phys. Rev. Lett. **66**, 3203 (1991).
[11]J. R. Schrieffer and P. A. Wolff, Phys. Rev. **149**, 491 (1966).
[12]R. M. Fye and D. J. Scalapino, Phys. Rev. B **44**, 7486 (1991).
[13]J. Kanamori, Prog. Theor. Phys. **30**, 275 (1963).
[14]M. C. Gutzwiller, Phys. Rev. Lett. **10**, 159 (1963); Phys. Rev. **134**, A923 (1964); **137**, A1726 (1965).
[15]D. Vollhardt, Rev. Mod. Phys. **56**, 99 (1984).
[16]T. M. Rice and K. Ueda, Phys. Rev. B **34**, 6420 (1986).
[17]G. Kotliar and A. E. Ruckenstein, Phys. Rev. Lett. **57**, 1362 (1986).
[18]A. M. Reynolds, D. M. Edwards, and A. C. Hewson, J. Phys. Condens. Matter **4**, 7589 (1992).
[19]A similar conclusion is obtained by using the $1/N$ expansion: P. Coleman, Phys. Rev. B **29**, 3035 (1984); and N. Read, D. M. Newns, and S. Doniach, *ibid.* **30**, 3841 (1984).
[20]H. Q. Lin, Phys. Rev. B **42**, 6561 (1990); **44**, 7151 (1991).
[21]R. M. Fye, Phys. Rev. B **41**, 2490 (1990).
[22]T. Nishino, Physica B (to be published).